Effect of Crystallization on the Lamellar Orientation in Thin Films of Symmetric Poly(styrene)-*b*-poly(L-lactide) Diblock Copolymer

Dongju Chen, Yumei Gong, and Tianbai He*

State Key Laboratory of Polymer Physics and Chemistry, Changchun Institute of Applied Chemistry, Chinese Academy of Sciences, Changchun, 130022, P. R. China

Fajun Zhang*

Institut fuer Angewandte Physik, Universitaet Tuebingen, 72076 Tuebingen, Germany

Received January 23, 2006; Revised Manuscript Received March 31, 2006

ABSTRACT: The effect of crystallization on the lamellar orientation of poly(styrene)-*b*-poly(L-lactide) (PS−PLLA) semicrystalline diblock copolymer in thin films has been investigated by atomic force microscopy (AFM), transmission electronic microscopy (TEM), and X-ray photoelectron spectroscopy (XPS). In the melt state, microphase separation leads to a symmetric wetting structure with PLLA blocks located at both polymer/substrate and polymer/air interfaces. The lamellar period is equal to the long period L in bulk determined by small-angle X-ray scattering (SAXS). Symmetric wetting structure formed in the melt state provides a model structure to study the crystallization of PLLA monolayer tethered on glassy ($T_c < T_{g,PS}$) or rubber ($T_c > T_{g,PS}$) PS substrate. In both cases, it is found that the crystallization of PLLA results in a "sandwich" structure with amorphous PS layer located at both folding surfaces. For $T_c \leq T_{g,PS}$, the crystallization induces a transition of the lamellar orientation from parallel to perpendicular to substrate in between and front of the crystals. In addition, the depletion of materials around the crystals leads to the formation of holes of $^1/_2L$, leaving the adsorbed monolayer exposure at the bottom of the holes. In contrast, the adsorbed monolayer on the substrate with thickness of $^1/_2L$ does not change in parallel orientation and thickness upon crystallization. When $T_c > T_{g,PS}$, no perpendicular lamellae and holes could be observed due to the high mobility of molecules.

Introduction

Block copolymers consist of chemically distinct blocks covalently connected at one end. Because of the immiscibility, block copolymers may pass through a disorder-to-order phase transition, depending on the value of χN, where χ is the Flory−Huggins interaction parameter and N is the degree of polymerization.[1−3a] Both theoretical and experimental studies have revealed abundant morphologies of segregated block copolymers including lamellae, gyroids, cylinders, and spheres, depending on the volume fraction of the block copolymer, f. Moreover, with the same material, different morphologies can be observed in response to the film preparation conditions,[3b] such as the application of external fields, type of solvent used, amount of solvent uptake, solvent evaporation rate, and film confinement conditions.

If one of the blocks is crystalline and the other is amorphous, the final state of semicrystalline diblock copolymer depends on the competition between three phase transitions, i.e., the order−disorder transition of the diblock copolymer, the crystallization of the crystallizable block, and the vitrification of the amorphous block.[4] In the past few decades, the bulk properties of many semicrystalline block copolymers have been extensively studied[4−12] and reviewed.[3a] Although a large body of work on bulk behavior of semicrystalline block copolymer has been done, investigation in thin films is just in the beginning.[13−23]

When a thin film of a symmetric diblock copolymer is in contact with a solid surface, preferential interactions between the blocks and the substrate result in two types of lamellar structures:[24−29] (a) symmetric structure if the same block segregates to both interfaces and (b) antisymmetric structure if each interface adsorbs different components. The film thickness (h) is quantized as $h = nL$ for symmetric system or $h = (n + {}^1/_2)L$ for antisymmetric system, where L is the bulk value of the copolymer lamellar period and n is an integer. If the initial film thickness does not fit these values, relief structures of islands or holes with a step height of L form on the surface of the thin films.[24−29] The large potential application of block copolymer thin films to future technologies stimulates intensively research activity on both fundamental and applied. Recent research is centering mainly on the control of thin film morphology.[30−32] Studies on the properties of semicrystalline block copolymer thin films have attracted much attention. Fundamentally, poly(ethylene oxide-*b*-butadiene) (PEO−PB) diblock copolymers in uniform lamellar films have been investigated as a model system for confined crystallization.[13−17] In these studies,[13,15−17] the PB blocks wetted the air interface, whereas PEO layer wetted the substrate, forming an antisymmetric lamellar structure. Crystallization of PEO layer was confined between two amorphous PB layers. In previous work,[18,19] we have studied the surface-induced ordering and crystallization behavior of a weakly segregated symmetric block copolymer poly(styrene-*b*-ϵ-caprolactone) (PS−PCL) in thin films. Surface-induced ordering resulted in antisymmetric lamellar structure with PS and PCL layer wetting air and substrate, respectively. We found that crystallization preferred to occur at the edge of islands or holes because the stretched PCL block therein could act as nucleation agents during polymer crystallization. Very recently, Fu and co-workers[20−22] have studied the interplay between phase separation and crystallization in a PS−PLLA thin film. Surface-induced ordering resulted in an

* To whom correspondence should be addressed. Tianbai He: e-mail tbhe@ciac.jl.cn; Fax +86 431 5262126; Tel +86 431 5262123. Fajun Zhang: e-mail fajun.zhang@uni-tuebingen.de; Fax +49 7071-29-5110; Tel +49 7071-29-78670.

10.1021/ma0601565 CCC: $33.50
Published on Web 05/13/2006

antisymmetric lamellar structure with PS and PLLA layers located at the air and substrate, respectively.

By far, most of the semicrystalline block copolymer thin films form antisymmetric lamellar structure, in which the free surface is always occupied by amorphous layer.[13,15−22] Less is known about the symmetric lamellar structure with crystalline layer on both interfaces. In fact, such symmetric lamellar structure might serve as a model system to study the crystallization of tethered chains on a free surface.

In this work, we have investigated thin films of a symmetric PS−PLLA diblock copolymer on supported silicon wafer. We found that the PLLA blocks segregated to both the substrate and the air interfaces upon annealing. The results of TEM and AFM illustrated that crystallization of the tethered PLLA layer could induce a lamellar orientation transition from parallel to perpendicular to the substrate. It provides a new way to tailor the morphology and structure of diblock copolymers thin films, which serve as templates for a wide range of technologies.

Experimental Section

Material and Film Preparation. The diblock copolymer, PS−PLLA, was purchased from Polymer Source, Inc. The number-average molecular weight (M_n) is 40 500 (PS: 21 000; PLLA: 19 500), and polydispersity is 1.1 characterized by gel permeation chromatography (GPC). The total degree of polymerization is $N = 473$ determined by ^{1}H NMR. The volume fractions of PS and PLLA are 0.51 and 0.49, respectively; thus, the copolymer is approximately symmetric. The volume fraction was calculated on the basis of the equation $f_{PS} = N^*_{PS}/(N^*_{PS} + N^*_{PLLA})$, with $N^*_{PS} + N^*_{PLLA} = N_{PS}(r_{PLLA}/r_{PS}) + N_{PLLA}(r_{PS}/r_{PLLA})$, where $r_{PS} = 1.047$ g/cm^3 and $r_{PLLA} = 1.245$ g/cm^3 are the densities of PS and amorphous PLLA, respectively.

Polymer films were prepared by spin-coating a solution of 5 mg/mL in chloroform onto freshly cleaned silicon wafer with native oxide layer at 2000 rpm for 30 s. All the wafers were cleaned in a mixture of H_2SO_4, H_2O_2, and H_2O (70/21/9 vol %) for 30 min at 120 °C, followed by extensive rinsing with deionized water. The cleaned wafers were dried in a stream of nitrogen and used immediately for the film deposition. The residual solvent was removed under vacuum for 24 h at room temperature. The film thickness was determined by ellipsometry and AFM after scratching with a blade. The initial film thickness is $h = 33 \pm 1$ nm. The samples were annealed at 180 °C under vacuum and then quenched to room temperature or preset temperatures for crystallization. The topography and structure of the resulting films were examined by atomic force microscopy (AFM), transmission electronic microscopy (TEM), and X-ray photoelectron spectroscopy (XPS).

Atomic Force Microscopy (AFM). Tapping mode AFM was conducted at ambient conditions using a SPA-300HVwith a SPI3800N controller (Seiko Instruments Industry Co., Ltd., Japan). Both height and phase images were recorded simultaneously using the retrace signal. Etched Si tips with a resonance frequency of ~70 kHz and a spring constant of about 2 N/m were used, and the scan rate was in the range from 1.0 to 2.0 Hz. Each scan line contains 256 pixels, and a whole image is composed of 256 scan lines.

Transmission Electronic Microscopy (TEM). TEM experiments were performed on JEOL 1011 TEM with an accelerating voltage of 100 kV. The polymer thin films were floated from the silicon wafers and quickly transferred to copper grids. A saturated KOH solution at ~90 °C was used to etch away the silicon oxide layer and release the film. This method has been used to separate polymer thin films from substrate without altering the properties of the films.[33] Gold was evaporated on the thin films for the calibration of the electron diffraction (ED) spacing. To avoid damage, the samples were not stained, and the contrast came from the difference of the electron density between PLLA and PS (380 and 340 nm^{-3} for amorphous PLLA and PS, respectively.)

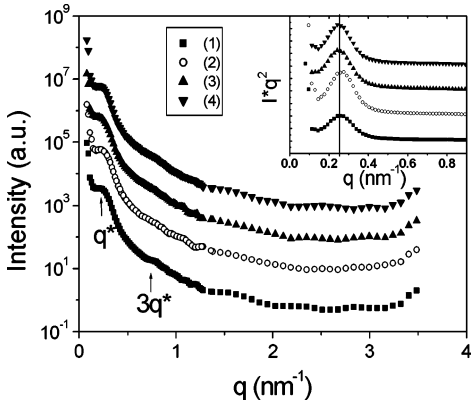

Figure 1. Room temperature SAXS profiles of PS−PLLA diblock copolymer sample quenched from ordered melt at 180 °C or isothermally crystallized at various temperatures from ordered melt: (1) 180 °C for 1 h, (2) 82 °C for 5 h, (3) 93 °C for 18 h, and (4) 115 °C for 42 h.

X-ray Photoelectron Spectroscopy (XPS). The surface chemical composition of thin films was determined with a VGESCALAB-MKII spectrometer with an Mg X-ray source. Pass energy of 20 eV was used to obtain the high resolution, and the takeoff angle of the X-ray source was 90°. The main chamber of the XPS instrument was maintained at 2.0×10^{-7} Pa during the spectral measurements. The relative photoelectron intensities of the C 1s peak (289 eV) were used to determine the composition of the upper layer of the polymer thin film.

Differential Scanning Calorimetry (DSC). The thermal behaviors of the PS−PLLA diblock copolymer were measured with a Perkin-Elmer Diamond DSC-7. The melting point of the PLLA blocks in PS−PLLA was around 165 °C. The glass transition temperatures of PLLA and PS were approximately 58 and 93 °C, respectively. All of the measurements were carried out at the heating rate of 10 °C/min. The relative crystallinity of PLLA was determined by the equation $W_c = \Delta H_m(t)/(W_E\ \Delta H_m f) = 32.8\%$, where W_E is the weight fraction of the PLLA block and ΔH_m is the melting enthalpy of 100 wt % crystalline PLLA (93 J/g).[10]

Small-Angle X-ray Scattering (SAXS) and Wide-Angle X-ray Diffraction (WAXD). Morphology and crystalline structure of PS−PLLA diblock copolymer in bulk were determined by SAXS and WAXD. Samples were first melt at 180 °C for 10 min and then quenched to room temperature to "freeze" the melt structure or the selected crystallization temperature. All the measurements were carried out at room temperature. SAXS was performed on an evacuated Kratky compact camera (Kratky PW1700 X-ray scatteractometer, Holand). The X-ray source is a sealed X-ray tube with copper anode working at 45 kV and 40 mA. The wavelength λ of Cu Kα is 0.154 nm. The primary data were plotted as the scattering intensity (I) vs the scattering vector, $q = 4\pi \sin\theta/\lambda$ (θ = scattering angle). WAXD spectra were obtained with a Rigaku D/max 2500V PC X-ray diffractometer (Japan) with a rotating-anode Cu Kα X-ray source working at 40 kV and 200 mA. The 2θ angle region ranged between 2° and 40° with a scanning rate of 5°/min.

Results and Discussion

1. Bulk Behavior of PS−PLLA Diblock Copolymer. In this section, the bulk behavior of PS−PLLA diblock copolymer is presented to compare with the results obtained in the following studies in thin films. The SAXS profiles of PS−PLLA diblock copolymer in both melt and crystalline states are shown in Figure 1. In the melt state the SAXS profile shows q^* and $3q^*$ as indicated by arrows in Figure 1, indicating the formation of lamellar structure via microphase separation. The absence of the $2q^*$ indicates that the thickness of the PLLA layer is similar to that of the PS layer. Lorentz corrected SAXS profiles are shown in the inset of Figure 1. The long period L can be

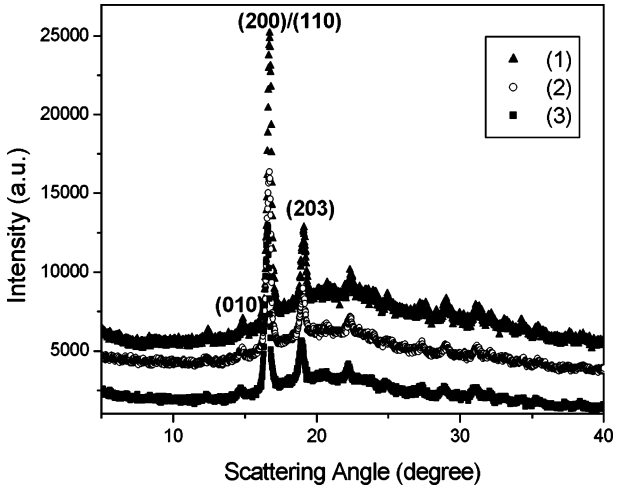

Figure 2. WAXD patterns of PS−PLLA diblock copolymer completely crystallized at various temperatures from ordered melt at 180 °C: (1) 82 °C for 5 h, (2) 93 °C for 18 h, and (3) 115 °C for 42 h.

calculated from the peak maximum using the Bragg·s equation; the sharp peak at $q^* \sim 0.253$ nm^{-1} corresponds to $L = 2\pi/q^* = 24.8 \pm 0.3$ nm, where q^* is the wave vector at the first order-peak. The scattering profiles of the samples crystallized at 82, 93, and 115 °C do not show significant change; the long periods are 24.5 ± 0.3, 25.6 ± 0.4, and 25.3 ± 0.4 nm, respectively.

The WAXD profiles of $T_c = 82$, 93, and 115 °C are displayed in Figure 2. Characteristic crystalline peaks of PLLA are found at $2\theta = 16.6°$ and 19.1°.[34,35] The peak positions are in good agreement with the reported unit cell parameters for PLLA (orthorhombic, $a = 1.06$ nm, $b = 0.61$ nm, and $c = 2.88$ nm).[34] The two main diffraction peaks located at $2\theta = 16.6°$ and 19.1° correspond to the (200)/(110) and (203) diffraction planes. The positions of crystal reflections do not change with crystallization temperature, which indicates that there are no significant distortions of the PLLA crystals, though they are confined within the amorphous PS layers.

Zalusky et al.[36] calculated interaction parameter between PLA and PS by $\chi(T) = 98.1/T - 0.112$, where T is the temperature in kelvin and χ is the Flory−Huggins segmental interaction parameter. Assuming that solubility parameters between PLA and PLLA are similar, the theoretical criterion of phase separation is $\chi(T_{ODT})N = 10.5$.[1−3a] The order−disorder transition temperature (T_{ODT}) of our system is calculated as $T_{ODT} = 458$ °C. Thus, the copolymer under the experimental condition is always in the phase-separated state. SAXS results (Figure 1) show that the long period of samples crystallized at various temperatures remains constant, which indicates that the crystallization does not destroy the lamellar morphology initially present. The crystallization of PLLA is confined within the layered framework formed during phase separation. Ho et al. also found that there was no significant change of the long period of PS−PLLA after crystallization, though the undulated morphology could be observed at temperature higher than the T_g of PS block.[10]

2. Topography of PS−PLLA Diblock Copolymer Thin Films in Melt State. Figure 3 shows the AFM images of thin films annealed at 180 °C for 10 min under vacuum and then quenched to room temperature. In all measurements, islands were observed on the surface after annealing. To reveal the thickness of the continuous film, a thin film was scratched before annealing. A typical AFM height image of scratched area and cross-section profile are shown in Figure 3. The cross-section analysis has been repeated many times, and the results are

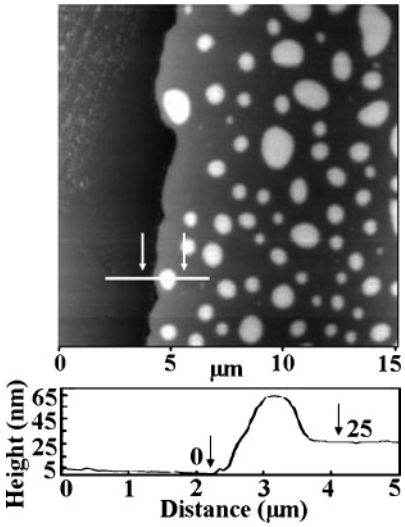

Figure 3. AFM height images and the corresponding cross-section line profiles of PS−PLLA diblock copolymer thin films in melt state. Thin film was scratched first and then annealed at 180 °C for 10 min.

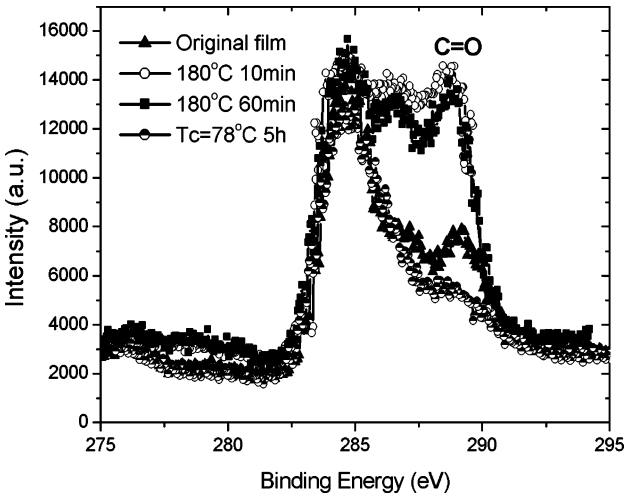

Figure 4. XPS C 1s spectra of PS−PLLA diblock copolymer: the initial thin film, the thin film annealed at 180 °C for 10 and 60 min, and crystallize at 78 °C for 5 h. The profiles were normalized on the peak of C−C bond with binding energy of 284 eV. The C 1s peak at 288.8 eV corresponds to the carbonyl group, which shifts slightly toward lower binding energy after annealing.

reproducible within the experimental error range. The thickness of the continuous film is 25 ± 1 nm, well in agreement with the long period $L = 24.8$ nm, obtained from SAXS measurement (Figure 1). The height of the islands above the continuous film larger than one period. Studies on islands by TEM (results not shown) indicate that the lamellae within islands are not parallel but perpendicular to the substrate. The detailed morphology and structure of islands will be discussed in another work. In this paper we will focus on the structure transition of the continuous film. On the basis of these results and the fact that the initial film thickness $L < h$ (33 ± 1 nm) $< {}^3/_2L$, we conclude that annealing the PS−PLLA diblock copolymer thin films gives a symmetric wetting structure.[24−29] XPS is used to determine the change of the surface composition before and after annealing. Figure 4 shows the profiles of relative photoelectron intensity of C 1s as a function of binding energy for a original film, films annealed at 180 °C for 10 and 60 min, and a film crystallized at 78 °C for 5 h after annealing at 180 °C for 10 min. The profiles have been normalized on the peak of C−C bond with a binding energy of 284 eV. The C 1s peak at 288.8 eV

corresponds to the carbonyl group, which shifts slightly toward lower binding energy after annealing. It is obvious that the relative intensity of C 1s peak increases after annealing, which indicates that the top layer is mainly composed of PLLA. Similar intensity profiles are obtained for thin films annealed at 180 °C for 10 and 60 min, indicative of a fast reorganization process. After crystallization, the relative intensity of carbonyl group even lower than that of the original film, which means the PS dominates on the surface of the solid film. This result will be further discussed in section 3.

Combined the results of Figure 3 and Figure 4, the continuous film formed via annealing is interpreted by a symmetric wetting structure with PLLA domains wetting the two interfaces, whereas the PS blocks segregate to the internal of thin films, and the lamellar period is equal to the long period L in bulk. Such structure is reasonable since the polar PLLA blocks prefer to wet the surface of the silicon wafer with native oxide layer and the phase with lower surface tension (PLLA) wet the air interface. As reported in the literature, the surface tensions of PLLA and PS at room temperature are 38.3 and 40.7 mN/m, respectively.[37,38] Recently, Fu et al. reported an antisymmetric wetting behavior of a low molecular weight PS−PLLA diblock copolymer thin films on supported silicon wafer surface.[20−22] The reason for this distinct behavior is unclear; however, since the surface tension values of PS and PLLA are so close to each other, the molecular weight dependence of surface tension might play an important role in it.[39]

3. Lamellar Orientation of PS−PLLA Diblock Copolymer Thin Films after Crystallization. The symmetric structure of PS−PLLA diblock copolymer thin films in melt state provides an ideal model to study crystallization of PLLA monolayer tethered on glassy or rubbery PS substrate by simply tuning the crystallization temperature. For all the subsequent experiments on crystallization, the thin films are first annealed at 180 °C for 10 min and then quenched to the selected T_c for crystallization. Once the crystallization is completed, the thin films are quenched to room temperature. The morphology and structure of thin films after crystallization at temperatures ranging from 70 to 100 °C are investigated by AFM (Figure 5) and TEM (Figure 6) at room temperature. Results of three typical crystallization temperatures are presented in Figure 5 and Figure 6, i.e., T_c = 78, 93, and 98 °C, corresponding to below, approach, and above the T_g of PS domains.

3.1. AFM Observations. Figure 5a,b shows the AFM images of $T_c = 78\ °C < T_{g,PS}$ for 5 h. Dendritic crystals filled the whole surface. Some small holes could be observed between the crystals, which were caused by the depletion of materials in front of the crystals. The cross-section line scan profile at the bottom of Figure 5a shows that the depth of small holes is about 12 nm close to $^1/_2L$. Figure 5b presents a high-magnification AFM phase image from the white box of Figure 5a. It is interesting to see that alternative perpendicular lamellae appear in the area between the crystals.

Increasing crystallization temperature to $T_c = 93\ °C \approx T_{g,PS}$ for 20 h (Figure 5c−e), the coverage of dendritic crystals on the surface decreased, while the size of depletion holes increased (Figure 5c). The alternative perpendicular lamellae are also observed in phase image (Figure 5d). The line scan profile clearly shows that the depth of the hole is about 13 nm $\sim {}^1/_2L$ (Figure 5c). The scratching experiment (Figure 5e) further demonstrates the existence of an adsorbed layer of $^1/_2L$ at the bottom of the holes. Fu et al. also observed the depletion induced the formation of holes with the depth of $^1/_2L$.[20−22] Therefore, crystallization of PLLA blocks only transformed the morphology

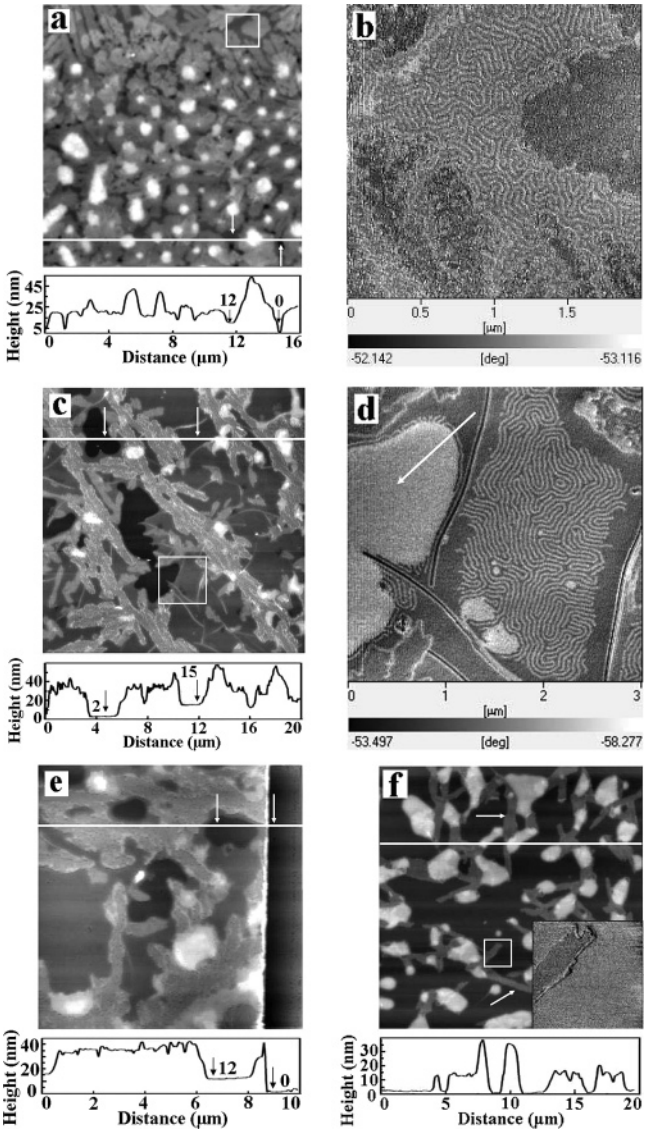

Figure 5. AFM images and the corresponding cross-section line profiles of PS−PLLA diblock copolymer thin films in crystalline state. (a) AFM height image, T_c = 78 °C for 5 h. (b) High-magnification phase image from the white frame in (a). (c) AFM height image, T_c = 93 °C for 20 h. (d) AFM phase image from the white frame in (c). (e) AFM height image, T_c = 93 °C for 20 h. (f) AFM height image, T_c = 98 °C for 24 h. The inset is a phase image at high magnification from the white frame.

of the top polymer layer with half period, leaving an adsorbed layer on the substrate.

The most interesting observations at both 78 and 93 °C are perpendicular lamellae in the area between the crystals as shown in Figure 5b,d. But no perpendicular lamellae could be observed within the hole (marked by white arrow in Figure 5d), indicating that the parallel lamellar structure is preserved in the absorbed monolayer. The perpendicular lamellar period at 78 and 93 °C are 38 ± 1 and 44 ± 1 nm, respectively. The lamellar period increases with crystallization temperature, but they are much larger than the long period in bulk (25 nm). In addition, the lamellar period does not show significant temperature dependence upon crystallization in bulk (Figure 1). The increase of lamellar period in block copolymer thin films upon crystallization has been reported in other groups.[15,16] However, the crucial distinction between thin film and bulk has never been reported so far. While we believe that the reduced confinement in thin films compared to bulk state plays the role on our observations,

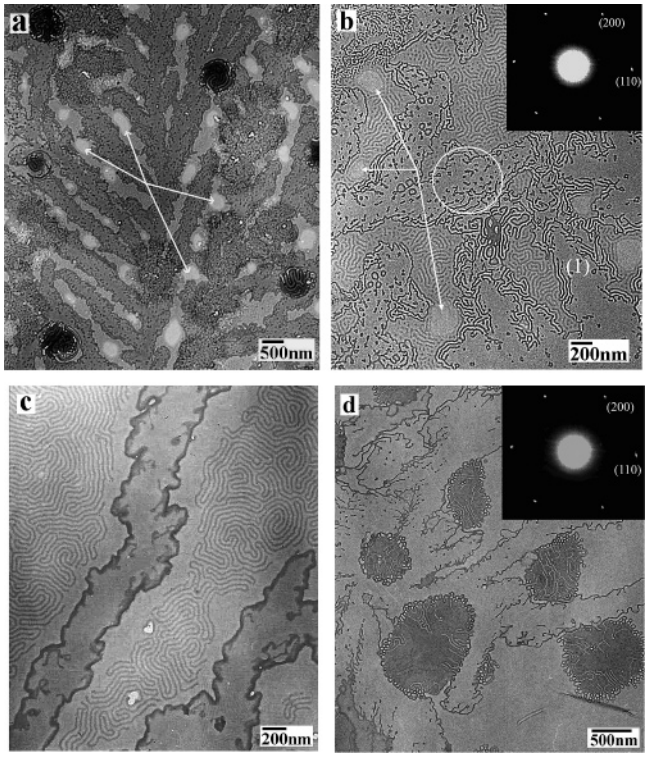

Figure 6. TEM images of morphology and structure in PS−PLLA diblock copolymer thin films after crystallization. (a) $T_c = 78$ °C for 5 h. (b) $T_c = 78$ °C for 5 h. The inset is selective-area ED pattern. (c) $T_c = 93$ °C for 20 h. (d) $T_c = 98$ °C for 24 h. The inset is selective-area ED pattern.

further investigation should be done in other systems in order to reveal the rule in it.

Further increasing the crystallization temperature, $T_c = 98$ °C > $T_{g,PS}$ for 24 h. (Figure 5f). The crystal growth rate at this temperature is very slow; only small crystals are observed around the islands as indicated by white arrows in Figure 5f. The depletion holes are rarely observed on the free surface. The high-magnification phase image (inset of Figure 5f) shows a smooth surface indicative of a parallel lamellar structure; no perpendicular lamellar structure could be observed in the area between crystals.

3.2. TEM Observations. The morphology and structure of thin films after crystallization are further characterized by TEM. Figure 6a shows a typical TEM image of $T_c = 78$ °C < $T_{g,PS}$. At high coverage of crystals, the holes between the crystals as indicated by the white arrows are confirmed. The contrast in the area of the holes is homogeneous, and no perpendicular lamellar structure can be observed. Figure 6b shows a high-magnification image. Here, the perpendicular lamellar structure can be observed not only in between the crystals but also at the edge of crystals. Though there are many perpendicular lamellae around the holes as marked by white arrows in Figure 6b; no perpendicular lamellae could be observed in the bottom of holes, indicating that the orientation of the absorbed lamellar layer of $^1/_2L$ at the substrate is parallel.

The region (1) labeled in Figure 6b is indicative of a well-developed crystal. The homogeneous contrast of the crystal surface indicates a parallel orientation within the crystal, i.e., a flat-on crystal. The XPS results (Figure 4) reveal the surface component of crystal. The relative intensity of carbonyl group is even lower than that of the original film, indicating that the PS component dominates on the free surface after crystallization. The inset of Figure 6b shows a selected-area electron diffraction pattern of the dendritic crystal, which indicates that the crystal is an α-modification and the chains are perpendicular to the substrate.[40] Many diffraction patterns for samples crystallized in the whole T_c range were obtained, and all shown the same diffraction patterns regardless of the crystallization temperature.

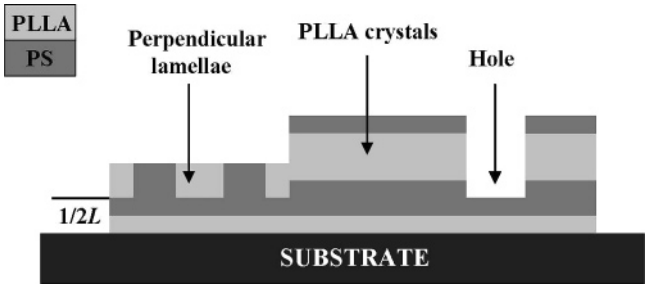

Figure 7. Schematic of the structure in PS−PLLA diblock copolymer thin film after crystallization.

At $T_c = 93$ °C ≈ $T_{g,PS}$ (Figure 6c), perfect perpendicular lamellae are observed. At $T_c = 98$ °C > $T_{g,PS}$ (Figure 6d) no perpendicular lamellar structure could be observed between crystals. These results are in good agreement with our AFM observations (Figure 5). Note that the perpendicular structure formed during crystallization could be easily converted to their original state, i.e., the parallel lamellar structure, by simply heating the samples higher than its melting point.

4. Origins of the Lamellar Orientation Transition. In sections 2 and 3, the morphology and structure of PS−PLLA semicrystalline diblock copolymer thin films in melt and crystalline states have been presented. In the melt state, PLLA layer wets both the polymer/air and polymer/substrate interfaces, forming a symmetric lamellar structure. The polymer chains reorganized during crystallization result in a "sandwich structure" with amorphous PS layer located at both folding surfaces. When T_c is below or approaches $T_{g,PS}$, the perpendicular lamellae are observed between crystals. The structure of thin film after crystallization in this temperature range is illustrated in Figure 7.

The resulting "sandwich" crystal structure (Figure 4) with amorphous PS layer located at both interfaces is energetically favored. Such "sandwich" structure has been observed in many semicrystalline diblock copolymers.[41,42] If the liquid layer (in melt state) transfers directly into two-layer crystalline state with PLLA crystals still on the top layer, the resulting solid structure is definitely energetically unfavorable, since the fold surface energy of PLLA crystals is very high.[22] It is shown in Figure 5a,c,e that when the PS flipping from sandwiched between PLLA layers to on top of the film, the crystal thickness increased to $1.5L = 36$ nm. It means that transformation to "sandwich" structure is associated with change in block chain folding. At a constant crystallization temperature (T_c), PLLA blocks have to crystallize with a constant crystalline stem thickness determined by the undercooling ($\Delta T = T_m - T_c$), no matter whether they are in a double layer at each side of the PS lamella or interdigitated in a single layer as sandwiched between two PS lamellae. When two layers of PLLA are on each side of the PS lamellae, PLLA blocks have to have fewer numbers of folds than they are interdigitated, since interdigitation of PLLA can double the number of folds provided the crystalline stem has the same length. As a result, few numbers of folds in double layers of PLLA will increase the tethering point density and thus induce overcrowding of the PS blocks to adopt an elongated conformation like a brush, which increases the overall system energy. Therefore, double-layer PLLA crystals are thermodynamically less stable than the sandwiched single-layer PLLA

crystal, and PS chains have to flip to the top of the film during/after PLLA crystallization.[43]

The formation of such "sandwich" crystal structure needs reorganization of the layer structure; i.e., half amount of the PS blocks have to move to the top of the crystals. When T_c is above $T_{g,PS}$, due to the high mobility of PS blocks large scale reorganization takes place, resulting in the formation of flat-on lamellar crystals. When T_c is below or approaches $T_{g,PS}$, the low mobility of PS blocks leads to partial perpendicular lamellae since the transformation of the PS blocks to the top layer is difficult. Consequently, both flat-on crystals and perpendicular lamellae could be observed. Obviously, the energy barrier of this transition is low because of the small difference on surface tension of PS and PLLA.[37,38] It should be noted that the glass transition temperature of PS $T_{g,PS}$ may decrease in ultrathin films.[44,45] Thus, mobility of the PS blocks in diblock copolymer thin film could be observed at the temperature below the apparent $T_{g,PS}$.

Conclusions

We have studied the morphology and the lamellar orientation of symmetric PS−PLLA diblock copolymer thin films in melt and crystalline states using AFM, XPS, and TEM. The lamellar structure phase-separated in the melt state, and the crystalline structure of PLLA blocks in bulk have been determined by SAXS and WAXD. The long period of the lamellar structure is $L = 24.8 \pm 0.3$ nm in melt and does not show significant change upon crystallization. The PLLA blocks crystallize into orthorhombic form, similar to that of PLLA homopolymer.

The initial film thickness is $1\ L < h < {}^3/_2L$ prepared by the spin-coating method. Annealing the films at 180 °C for as little as 10 min, surface-induced ordering, and microphase separation result in a symmetric parallel lamellar structure with thickness of L. AFM and XPS results show that PLLA blocks locate at both polymer/substrate and polymer/air interfaces. Such a symmetric wetting behavior is attributed to the polar interaction between PLLA and substrate and the relatively lower surface tension of PLLA.

Crystallization of the top PLLA layer from the ordered melt state at T_c below, approach, and above the $T_{g,PS}$ gives a "sandwich" structure with amorphous PS layer located at both folding surfaces as concluded from the results of AFM, TEM, and XPS. Compared with the parallel lamellar structure formed in the melt state, the crystal growth process accompanied by the reorganization of polymer chains resulted in the transition of the lamellar structure from parallel to perpendicular in between and front of the crystals at $T_c \leq T_{g,PS}$. Depletion of copolymer chains around the crystals led to the formation of holes of ${}^1/_2L$, leaving the adsorbed monolayer at the bottom of the holes. In contrast, the adsorbed monolayer on the substrate with thickness of ${}^1/_2L$ does not change in parallel orientation and thickness upon cooling. When $T_c > T_{g,PS}$, no perpendicular lamellae and holes could be observed due to the high mobility of molecules.

Acknowledgment. The authors thank Prof. Günter Reiter (Institute de Chimie des Surfaces et Interfaces, Mulhouse, France) and Dr. Jun Fu (Max Planck Institute for Polymer Research, Mainz, Germany) for helpful discussion and constructive suggestions.This work is supported by National Science Foundation of China (20234020) and the Chinese Academy of Sciences (KJCX2-SW-H07) and subsidized by National Basic Research Program of China (2005CB6238).

References and Notes

(1) Bates, F. S.; Fredrickson, G. H. *Annu. Rev. Phys. Chem.* **1990**, *41*, 525.
(2) Leibler, L. *Macromolecules* **1980**, *13*, 1602.
(3) (a) Hamley, I. W. *The Physics of Block Copolymer*; Oxford University Press: New York, 2000. (b) Cited refs 3−16 by: Gong, Y.; Huang, H.; Hu, Z.; Chen, Y.; Chen, D.; Wang, Z.; He, T. *Macromolecules* **2006**, *39*, 3369.
(4) (a) Zhu, L.; Chen, Y.; Zhang, A.; Calhoun, B. H.; Chun, M.; Quirk, R. P.; Cheng, S. Z. D.; Hsiao, B. S.; Yeh, F.; Hashimoto, T. *Phys. Rev. B* **1999**, *60*, 10022. (b) Zhu, L.; Calhoun, B. H.; Ge, Q.; Quirk, R. P.; Cheng, S. Z. D.; Thomas, E. L.; Hsiao, B. S.; Yeh, F.; Liu, L.; Lotz, B. *Macromolecules* **2001**, *34*, 1244. (c) Zhu, L.; Cheng, S. Z. D.; Calhoun, B. H.; Ge, Q.; Quirk, R. P.; Thomas, E. L.; Hsiao, B. S.; Yeh, F.; Lotz, B. *J. Am. Chem. Soc.* **2000**, *122*, 5957; *Polymer* **2001**, *42*, 5829.
(5) (a) Hamely, I. W.; Fairclough, J. P. A.; Bates, F. S.; Ryan, A. J. *Polymer* **1998**, *39*, 1429. (b) Mai, S. M.; Fairclough, J. P. A.; Viras, K.; Gorry, P. A.; Hamley, I. W.; Ryan, A. J.; Booth, C. *Macromolecules* **1997**, *30*, 8392.
(6) (a) Hamely, I. W.; Fairclough, J. P. A.; Terrill, N. J.; Ryan, A. J.; Lipic, P. M.; Bates, F. S.; Towns-Andrews, E. *Macromolecules* **1996**, *29*, 8835. (b) Hamely, I. W.; Fairclough, J. P. A.; Ryan, A. J.; Bates, F. S. Towns-Andrews, E. *Polymer* **1996**, *37*, 4425.
(7) (a) Douzinas, K. C.; Cohen, R. E. *Macromolecules* **1992**, *25*, 5030. (b) Cohen, R. E.; Bellare, A.; Drzewinski, M. A. *Macromolecules* **1994**, *27*, 2321. (c) Kofinas, P.; Cohen, R. E. *Macromolecules* **1994**, *27*, 3002.
(8) (a) Quiram, D. J.; Register, R. A.; Marchand, G. R.; Adamson, D. H. *Macromolecules* **1998**, *31*, 4891. (b) Quiram, D. J.; Register, R. A.; Marchand, G. R.; Ryan, A. J. *Macromolecules* **1997**, *30*, 4551, 8338.
(9) (a) Loo, Y. L.; Register, R. A.; Ryan, A. J.; Dee, G. T. *Macromolecules* **2001**, *34*, 8968. (b) Loo, Y. L.; Register, R. A.; Ryan, A. J. *Macromolecules* **2002**, *35*, 2365. (c) Loo, Y. L.; Register, R. A.; Ryan, A. J. *Phys. Rev. Lett.* **2000**, *84*, 4120. (d) Loo, Y. L.; Register, R. A.; Adamson, D. H. *Macromolecules* **2000**, *33*, 8361.
(10) Ho, R.; Lin, F.; Tsai, C.; Lin, C.; Ko, B. *Macromolecules* **2004**, *37*, 5985.
(11) Chen, H. L.; Li, H. C.; Huang, Y. Y.; Chiu, F. C. *Macromolecules* **2002**, *35*, 2417.
(12) Balsamo, V.; Gil, G.; Urbina de Navarro, C.; Hamley, I. W.; von Gyldenfeldt, F.; Abetz, V.; Canizales, E. *Macromolecules* **2003**, *36*, 4515. (b) Balsamo, V.; Urbina de Navarro, C.; Gil, G. *Macromolecules* **2003**, *36*, 4507.
(13) de Jeu, W. H. In Reiter G., Sommer, J.-U., Eds.; *Polymer Crystallization: Observations, Concepts and Interpretations;* Springer: Berlin, 2003; pp 196−207.
(14) (a) Reiter, G.; Castelein, G.; Hoerner, P.; Riess, G.; Blumen, A.; Sommer, J. U. *Phys. Rev. Lett.* **1999**, *83*, 3844. (b) Reiter, G.; Castelein, G.; Hoerner, P.; Riess, G.; Sommer, J. U.; Floudas, G. *Eur. Phys. J. E* **2000**, *2*, 319.
(15) (a) Reiter, G.; Vidal, L. *Eur. Phys. J. E* **2003**, *12*, 497. (b) Reiter, G.; Castelein, G.; Sommer, J. U. *Phys. Rev. Lett.* **2001**, *87*, 226101.
(16) (a) Opitz, R.; Lambreva, D. M.; de Jeu, W. H. *Macromolecules* **2002**, *35*, 6930. (b) Lambreva, D. M.; Opitz, R.; Reiter, G.; Frederik, P. M.; de Jeu, W. H. *Polymer* **2005**, *46*, 4868.
(17) (a) Hong, S.; MacKnight, W. J.; Russell, T. P.; Gido, S. P. *Macromolecules* **2001**, *34*, 2398; *Macromolecules* **2001**, *34*, 2876.
(18) Zhang, F.; Chen, Y.; Huang, H.; Hu, Z.; He, T. *Langmuir* **2003**, *19*, 5563.
(19) Zhang, F.; Huang, H.; Hu, Z.; Chen, Y.; He, T. *Langmuir* **2003**, *19*, 10100.
(20) Fu, J.; Luan, B.; Yu, X.; Cong, Y.; Li, J.; Pan, C.; Han, Y.; Yang, Y.; Li, B. *Macromolecules* **2004**, *37*, 976.
(21) Fu, J.; Cong, Y.; Li, J.; luan, B.; Pan, C.; Han, Y. *Macromolecules* **2004**, *37*, 6918.
(22) Fu, J.; Luan, B.; Pan, C.; Han, Y. *Macromolecules* **2005**, *38*, 5118.
(23) (a) De Rosa, C.; Park, C.; Lotz, B.; Wittmann, J. C.; Fetters, L. J.; Thmoas, E. L. *Macromolecules* **2000**, *33*, 4871. (b) Park, C.; De Rosa, C.; Lotz, B.; Thmoas, E. L. *Macromol. Chem. Phys.* **2003**, *204*, 1514.
(24) (a) Russell, T. P.; Coulon, G.; Deline, V. R.; Miller, D. C. *Macromolecules* **1989**, *22*, 4600. (b) Bassereau, P.; Brodbreck, D.; Russell, T. P.; Brown, H. R.; Shull, K. R. *Phys. Rev. Lett.* **1993**, *70*, 1716. (c) Mayes, A. M.; Russell, T. P.; Bassereau, P.; Baker, S. M.; Smith, G. S. *Macromolecules* **1994**, *27*, 749. (d) Cai, Z.; Huang, K.; Montano, P. A.; Russell, T. P.; Bai, J. M.; Zajac, G. W. *J. Chem. Phys.* **1993**, *98*, 2376.
(25) Grim, P. C. M.; Nyrkova, I. A.; Semenov, A. N.; ten Brinke, G.; Hadziioannou, G. *Macromolecules* **1995**, *28*, 7501.
(26) Maaloum, M.; Ausserre, D.; Chatenay, D.; Gallot, Y. *Phys. Rev. Lett.* **1993**, *70*, 2577.

(27) Sikka, M.; Singh, N.; Karim, A.; Bates, F. S.; Satija, S. K.; Majkrzak, C. F. *Phys. Rev. Lett.* **1993**, *70*, 307.
(28) (a) Coulon, G.; Daillant, J.; Collin, B.; Benattar, J. J.; Gallot, Y. *Macromolecules* **1993**, *26*, 1582. (b) Coulon, G.; Russell, T. P.; Deline, V. R.; Green, P. F. *Macromolecules* **1989**, *22*, 2581.
(29) Pickett, G. T.; Witten, T. A.; Nagel, S. R. *Macromolecules* **1993**, *26*, 3194.
(30) Fasolka, M. J.; Mayes, A. M. *Annu. Rev. Mater. Res.* **2001**, *31*, 323.
(31) Krausch, G. *Mater. Sci. Eng.* **1995**, *R14*, 1.
(32) Takahashi, K.; Sawai, D.; Yokoyama, T.; Kanamoto, T.; Hyon, S. H. *Polymer* **2004**, *45*, 4969.
(33) (a) Liu, Y.; Zhao, W.; Zheng, X.; Rafailovich, M. H.; Sokolov, J. *Macromolecules* **1994**, *27*, 4000. (b) Liu, Y.; Rafailovich, M. H.; Sokolov, J. *Macromolecules* **1996**, *29*, 899.
(34) Hoogsteen, W.; Postema, A. R.; Pennings, A. J.; Brinke, G.; Zugenmaier, P. *Macromolecules* **1990**, *23*, 634.
(35) Kim, K.; Chung, S.; Chin, I.; Kim, M.; Yoon, J. *J. Appl. Polym. Sci.* **1999**, *72*, 341.
(36) Zalusky, A. S.; OlayoValles, R.; Wolf. J. H.; Hillmyer, M. A. *J. Am. Chem. Soc.* **2002**, *124*, 12761.
(37) (a) Murphy, W. L.; Mooney, D. J. *J. Am. Chem. Soc.* **2002**, *124*, 1910. (b) Irvine, D. J.; Ruzette, A. V. G.; Mayes, A. M.; Griffith, L. G. *Biomacromolecules* **2001**, *2*, 545.
(38) Green, P. F.; Thomas, M.; Christensen, T. M.; Russell, T. P. *Macromolecules* **1989**, *22*, 2189.
(39) Dee, G. T.; Sauer, B. B. *Adv. Phys.* **1998**, *47*, 161.
(40) (a) Abe, H.; Kikkawa, Y.; Inoue, Y.; Doi, Y. *Biomacromolecules* **2001**, *2*, 1007. (b) Iwata, T.; Doi, Y. *Macromolecules* **1998**, *31*, 2461.
(41) Lin, E. K.; Gast, A. P. *Macromolecules* **1996**, *29*, 4432.
(42) Chen, W. Y.; Li, C. Y.; Zheng, J. X.; Huang, P.; Zhu, L.; Ge, Q.; Quirk, R. P.; Lotz, B.; Deng, L.; Wu, C.; Thomas, E. L.; Cheng, S. Z. D. *Macromolecules* **2004**, *37*, 5292.
(43) The authors very appreciate reviewer giving such profound understanding.
(44) Keddie, J. A.; Jones, R. A. L.; Cory, R. A. *Faraday Discuss.* **1994**, *98*, 219.
(45) Tsui, O. K. C.; Zhang, H. F. *Macromolecules* **2001**, *34*, 9139.

MA0601565